ELSEVIER

Physica C 319 (1999) 219–228

PHYSICA C

Crystal structure of β-ZrNCl refined from X-ray powder diffraction data, electronic band structures of β-ZrNCl and superconducting Li_xZrNCl

S.Ya. Istomin [*,1], J. Köhler, A. Simon

Max-Planck-Institut für Festkörperforschung, Heisenbergstrasse 1, D-70569 Stuttgart, Germany

Received 10 March 1999; accepted 30 April 1999

Abstract

β-ZrNCl was prepared using a new synthetic route via thermal decomposition of $(NH_4)_2ZrCl_6$. The crystal structure of β-ZrNCl was refined using X-ray powder diffraction data ($R\bar{3}m$, $a = 3.60388(4)$, $c = 27.6719(4)$, $R_I = 0.049$, $R_P = 0.120$). The electronic band structure of β-ZrNCl and the previously reported superconducting $Li_{0.16}ZrNCl$ was calculated by Extended Hückel and LMTO methods. The results of the band structure calculation show that the nature of superconductivity in Li_xZrNCl is rather related to the 3D analogue ZrN than to copper based high-temperature superconductors.

PACS: 71.20; 61.10N; 61.66F

Keywords: Band structure; X-ray diffraction; Crystal structure; Synthesis; Layered nitride

1. Introduction

The discovery of superconductivity in layered complex copper oxides has also induced an extensive search for new superconductors among non-copper based reduced transition metal compounds. Recently, the electron-doped nitride chlorides of Zr and Hf with formulae Li_xMNCl, M = Zr, Hf have been discovered which exhibit superconductivity at 13 and 25.5 K, respectively [1–3]. They are of special interest because of their 2D character similar to the complex copper oxides. β-ZrNCl was synthesised for the first time by Juza and Hendersen [4] by ammonolysis of $ZrCl_4$. Ohashi et al. [5] developed a new synthetic route for the preparation of β-ZrNCl by direct reaction of Zr metal or ZrH_2 with NH_4Cl vapour. On the basis of X-ray powder diffraction data, Juza and Friedrichsen [6] proposed a layered structure for β-ZrNCl with close packing of Cl atoms and N atom layers with Zr atoms occupying octahedral voids. Only recently, several groups could show on the basis of

* Corresponding author. Tel.: +49-711-6891647; fax: +49-711-6891091; E-mail: istomin@simaix.mpi-stuttgart.mpg.de
[1] Permanent address: Department of Chemistry, Moscow State University, 119899 Moscow, Russia.

0921-4534/99/$ - see front matter
PII: S0921-4534(99)00298-1

refined powder data that β-ZrNCl crystallises in the SmSI type structure [7–9]; however, the reported atomic parameters vary largely.

In the present work we report on a new route for the preparation of β-ZrNCl. The crystal structure of β-ZrNCl has been refined from X-ray powder diffraction data and is discussed in comparison to the structural data obtained by other authors. The electronic band structures of β-ZrNCl and the intercalated superconducting $Li_{0.16}ZrNCl$ [8] with a different stacking sequence of the Zr–N layers have been calculated and are analysed for the first time.

2. Experimental

β-ZrNCl was prepared by thermal decomposition of $(NH_4)_2ZrCl_6$. $(NH_4)_2ZrCl_6$ as starting material was synthesised from $ZrCl_4$ (Alfa, 99.5%) and NH_4Cl (Merck, 99.8%) by a procedure which was described earlier [10] but slightly modified. A stoichiometric mixture of the educts was mixed in a dry box under Ar and filled into a Schlenk tube. After thermal treatment at 400°C for 4 h, the mixture was sealed in an evacuated Duran glass ampoule. One end of the ampoule with the mixture was placed at 400°C while another was held at approximately 100°C. The $(NH_4)_2ZrCl_6$ had transported to the colder end of the ampoule after 12 h.

$(NH_4)_2ZrCl_6$ is known to sublime at temperatures above 400°C while it decomposes with a high conversion rate at higher temperatures. Consequently, a special procedure had to be developed for the quantitative decomposition of $(NH_4)_2ZrCl_6$ into β-ZrNCl. $(NH_4)_2ZrCl_6$ was placed at the end of a long silica ampoule filled with Ar and was put into a two-zone furnace. In order to supply a volume for the gases formed during the decomposition of the $(NH_4)_2ZrCl_6$ an Ar-filled rubber ball was placed at one end of the open ampoule. The temperature of the empty zone (I) was increased to 750°C while the temperature of the zone (II) with sample

Table 1
Crystal data for β-ZrNCl

Empirical formula	ZrNCl
Formula weight [g/mol]	140.68
Temperature [K]	293(2)
Wavelength, $CuK\alpha_1$ [Å]	1.54060
Crystal system	trigonal
Space group, formula units	$R\bar{3}m$ (166), 6
Unit cell dimensions [Å]	$a = 3.60388(4)$, $c = 27.6719(4)$
Cell volume [Å^3]	311.25
$F(000)$ (electrons)	384.0
Absorption coefficient	514.17 cm^{-1}
Calculated density [g/cm^3]	4.503
Sample dimension	0.2 mm glass capillary
Instrument	Stoe STADI powder diffractometer $CuK\alpha_1$ radiation, Ge monochromator
Step length (2θ)	0.02°
Texture	[001] 0.271(1)
Refined absorption parameter	1.46
Mode of refinement	Full profile
Number of free parameters	9
2θ and $\sin\theta/l$ (max)	92.82° and 0.47
Goodness-of-fit on F^2	0.300
R (intensity)	0.049
R (profile)	0.120
Scale factor	0.379

Table 2
Positional and displacement parameters for β-ZrNCl

Atom	Position	z	B [Å^2]
Zr	6c	0.1194(1)	0.27(4)
Cl	6c	0.3868(1)	0.40(8)
N	6c	0.2039(3)	1.00

was first kept at 200°C and then gradually increased to support a slow sublimation of the $(NH_4)_2ZrCl_6$. Sublimed $(NH_4)_2ZrCl_6$ passed through the hot temperature zone (I) and decomposed quantitatively into β-ZrNCl. For a complete decomposition, the temperature of both zones were kept at 750°C for 2 h followed by a subsequent cooling to room temperature. β-ZrNCl was found as light yellow-green deposit on the walls of the ampoule in zone (I). Finally, the freshly prepared β-ZrNCl was purified by chemical transport at 850°C [5,11].

Powder samples of β-ZrNCl obtained in such way are stable against moisture. The atomic ratio Zr/Cl/N found for β-ZrNCl is 1:1:1 according to an EDX analysis and no oxygen could be detected. It is frequently argued that ZrNCl could contain small amounts of hydrogen, especially if it is prepared from Zr metal or ZrH_2 as starting material [12]. Therefore, we have analysed our ZrNCl sample on a possible H content with hot extraction and a silver contact at 850°C. However, we found it to be negligibly small ($< 0.001\%$).

Crystals of β-ZrNCl are extremely thin transparent plates which are too small to show reflections on a Laue or a precession camera. Therefore β-ZrNCl was examined by X-ray powder diffraction. The data were collected using a STOE STADI-P powder diffractometer ($CuK\alpha_1$ radiation, Ge monochromator) equipped with a mini-PSD detector, using a rotating sample in a Debye–Scherrer mode (diameter of the glass capillary — 0.2 mm). The refinement of the crystal structure was performed with the CSD program package [13]. The R_P value is relatively high compared to other programs as in CSD it is calculated after subtraction of the background from observed intensities [14]. Other details of the structural investigation are given in Table 1.

All reflections could be indexed with a hexagonal unit cell $a = 3.604$ Å and $c = 27.672$ Å. Starting values of the atomic coordinates for the refinement of β-ZrNCl in $R\bar{3}m$ were taken from Shamato et al. [8]. A first refinement of the structure with fixed atomic positions led to $R_I \sim 0.3$. Taking into account the layered character of the structure of β-ZrNCl, preferred orientation of the crystallites along [001] had to be anticipated. In fact, the refinement of the texture parameter along [001] led to a dramatic decrease of R_I down to ~ 0.1. The final R factors were $R_I = 0.049$, $R_P = 0.120$. The value of the displacement parameter for N was slightly negative, and it was therefore fixed at 1 Å^2 during the final refinement. It should be noted that this procedure does not change either the atomic coordinates or interatomic distances. Final atomic coordinates and thermal

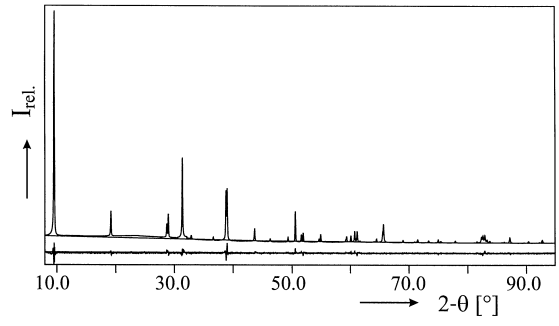

Fig. 1. Rietveld refinement of the crystal structure of β-ZrNCl. Observed diffraction pattern (upper curve) and difference between calculated and observed intensities (lower curve).

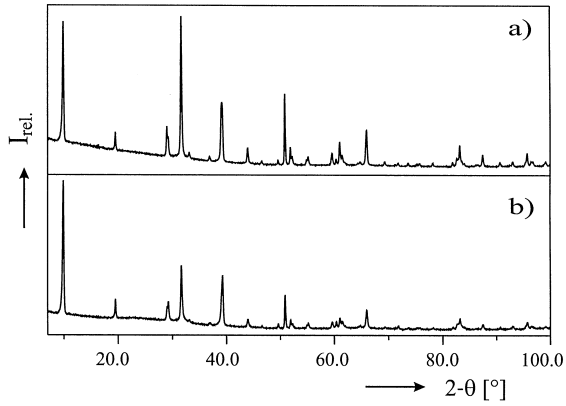

Fig. 2. Measured diffraction pattern of (a) a powder sample of β-ZrNCl after heat treatment in vacuum (10^{-6} Torr, 850°C) and (b) a powder sample of β-ZrNCl.

parameters are given in Table 2. Observed, calculated and difference X-ray diffraction intensities for β-ZrNCl are shown in Fig. 1. It is remarkable that the preferred orientation of the crystallites of a ZrNCl sample prepared as described above disappears completely after heat treatment in vacuum (10^{-6} Torr, 850°C), as depicted in Fig. 2. According to EDX analysis, the Zr/N/Cl ratio of such a ZrNCl sample is preserved and no weight loss was detected. The Rietveld refinement of the corresponding powder data did not result in a significant shift of the atomic parameters compared to the parameters given in Table 2.

3. Discussion of the structure

β-ZrNCl is isostructural to SmSI and its structure can be derived from ZrCl [15] by insertion of a double layer of N atoms between Zr atom layers. The structure can be described in terms of a close packing with 12 layers of N atoms and Cl atoms of the 1 s-type model, (I), stacking $(hcch)_3$:

$Cl_A(Zr_c)$	N_B	$N_C(Zr_b)$	Cl_A	$Cl_C(Zr_b)$	N_A	$N_B(Zr_a)$	Cl_C	$Cl_B(Zr_a)$	N_C	$N_A(Zr_c)$	Cl_B
h	c	c	h	h	c	c	h	h	c	c	h

(I)

It should be noted that the Cl atoms layers are packed in hexagonal sequence (h) while the N atoms are packed in a cubic manner (c). One can predict another model, (II), where the sequence of Cl atom layers is cubic (c) while the N atom layers pack hexagonally:

$N_A(Zr_c)$	Cl_B	$Cl_C(Zr_b)$	N_A	$N_C(Zr_b)$	Cl_A	$Cl_B(Zr_a)$	N_C	$N_B(Zr_a)$	Cl_C	$Cl_A(Zr_c)$	N_B
h	c	c	h	h	c	c	h	h	c	c	h

(II)

Several groups discussed the structure and bonding in β-ZrNCl [2,16] on the basis of model (II). However, this model should be excluded since the Zr atoms within the same ClNNCl block stack upon one another resulting in short distances $d_{Zr-Zr} \sim 2.75$ Å which is unrealistic for tetravalent Zr.

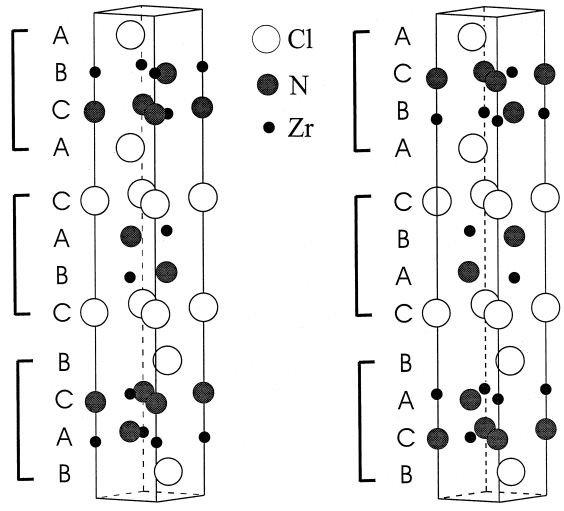

Fig. 3. Crystal structures of β-ZrNCl (left) and $Li_{0.16}ZrNCl$ (right) (only the Zr–N–Cl framework is shown). The different stacking sequence of N and Cl is graphically emphasised.

Finally, one can propose one more structural model for β-ZrNCl. This model (III), 3s type, can be derived from model (I) by changing the sequence of the N atom layers within the same ClNNCl block which leads to the following cubic sequence of close packed layers:

$$\begin{array}{cccccccccccc} Cl_A(Zr_b) & N_C & N_B(Zr_c) & Cl_A & Cl_C(Zr_b) & N_B & N_A(Zr_c) & Cl_C & Cl_B(Zr_a) & N_A & N_C(Zr_c) & Cl_B \\ c & c & c & c & c & c & c & c & c & c & c & c \end{array} \quad \text{(III)}$$

According to our refinement, β-ZrNCl crystallises in model (I) and there is no indication for the presence of a different or mixed stacking of the layers as it is found for, e.g., $TbClD_x$ ($x \sim 0.8$) [17]. However, the intercalation of β-ZrNCl with Li induces a shift of the slabs resulting in structure of Li_xZrNCl [8] with the slabs packed as in model (III). Such a transition from the so-called 1s to 3s type structure is also observed in other halides such as $Y_2Br_2C_2$ after intercalation with small alkali metal atoms (Li, Na) [18].

In the structure of β-ZrNCl (Fig. 3), Zr atoms are surrounded by three N ($d_{Zr-N} = 2.099(1)$ Å) and three Cl atoms ($d_{Zr-Cl} = 2.766(1)$ Å) from the neighbouring layer forming a distorted octahedron, see Table 3.

Table 3
Selected interatomic distances [Å] for β-ZrNCl and $Li_{0.16}ZrNCl$

	β-ZrNCl	β-ZrNCl	β-ZrNCl	β-ZrNCl	$Li_{0.16}ZrNCl$
Reference	(this work)	[7]	[9]	[8]	[8]
Radiation	X-rays	X-rays	X-rays	Neutrons	Neutrons
Temperature	298 K	298 K	298 K	15 K	15 K
Zr–Zr[a]	3.344(1)	3.355(3)	3.351(4)	3.272(1)	3.100(1)
Zr–N	2.099(1)	2.086(1)	2.125(6)	2.113(8)	2.083(2)
Zr–N′	2.339(9)	2.492(1)	2.170(3)	2.136(3)	2.045(1)
Zr–Cl	2.766(2)	2.754(3)	2.755(4)	2.769(2)	2.909(8)

[a] Interlayer distances.

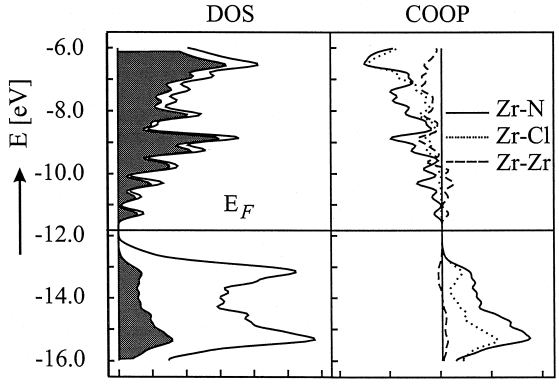

Fig. 4. Total density of states (DOS) together with the Zr centered states (black) and crystal orbital overlap population (COOP) curves for the Zr–N, Zr–Cl and Zr–Zr interactions in β-ZrNCl.

Additionally, another N atom from the adjacent N atom layer is coordinating the Zr atom at a distance of 2.339(9) Å resulting in a mono-capped trigonal $ZrCl_3N_4$-antiprism. However, the structural data of β-ZrNCl determined at room temperature by other authors deviate significantly from our data. [2] As shown in Table 3, there are only small differences between the Zr–Zr distances (3.344 to 3.355 Å) and the Zr–Cl distances (2.766 to 2.754 Å). The same holds for the Zr–N distances within one layer (2.086 to 2.125 Å) but the distance from Zr atom to the N atom of an adjacent layer ranges from 2.17 Å to 2.49 Å. This deviation might probably be due to hydrogen contamination of the differently prepared β-ZrNCl samples [12] or be due to a mixing of 1s and 3s stacking of the $[ClZr_2N_2Cl]$ slabs.

4. Band structure calculations

Two papers have addressed the electronic band structure of β-ZrNCl [16,19]. However, the calculations of the band structures were performed with positional parameters for β-ZrNCl corresponding to models (II) and (III) described above, which are obviously in error. Therefore, we have performed band structure calculations on the basis of the Extended Hückel method [20–25] for β-ZrNCl (positional parameters of this work) and for the superconducting $Li_{0.16}ZrNCl$ based on the positional parameters of [8]. [3]

The lowest unoccupied band in β-ZrNCl at about −11.5 eV is mostly Zr centered, see Fig. 4. The COOP curve indicates that there are states above the Fermi level, which have significant Zr–Zr bonding and Zr–N antibonding character whereas the Zr–Cl antibonding contribution is negligible. In Li intercalated ZrNCl, in spite of a different stacking sequence of the Zr–N layers, the band structure is basically preserved, see Fig. 5. In the superconducting phase $Li_{0.16}ZrNCl$, there is one more electron per unit cell ($Z = 6$ for β-ZrNCl) and therefore, the band corresponding to the lowest unoccupied band of ZrNCl is partially occupied. The Zr–Zr distance in $Li_{0.16}ZrNCl$ is significantly shortened in comparison to β-ZrNCl (Table 3) which is in accordance with Zr–Zr bonding which can be detected in the enlarged part of Fig. 5.

[2] The data obtained at 4 K should be taken into account.

[3] Parameters used in the EH calculations: atomic orbital energies: H_{ij} [eV] (coefficients ζ_1) for F: 2s −40.185 (2.425), 2p −18.5 (2.425); Ti: 4s −6.08 (1.500), 4p −3.85 (1.500), 3d −10.78 (4.55). Double ζ-functions were used for Ti: 3d C_1 0.4206, ζ_2 1.40 and C_2 0.7839.

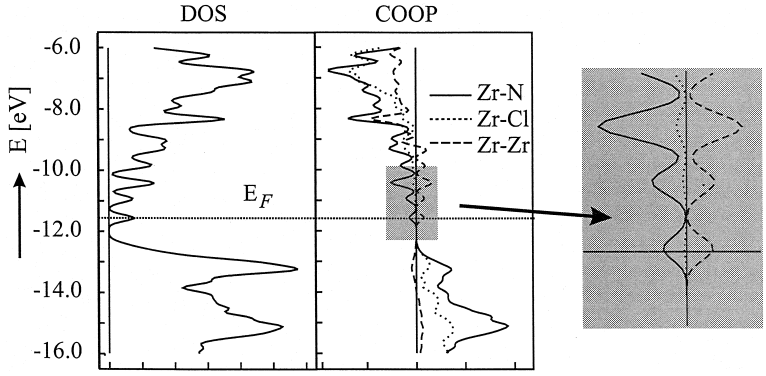

Fig. 5. Total density of states (DOS) and crystal orbital overlap population (COOP) curves for the Zr–N, Zr–Cl and Zr–Zr interactions in $Li_{0.16}ZrNCl$. An enlarged segment of COOP around the Fermi level is inserted.

In the intercalated compound, there is no van der Waals gap between the sheets of Cl atoms as they are bridged via Li atoms. As a consequence, in $Li_{0.16}ZrNCl$ the Zr–Cl distances are much longer, 2.91 Å instead of 2.77 Å. This leads to a shortening of the Zr–N distances, see Table 3. It is remarkable that the Zr–Zr bonding and Zr–N antibonding states are partially occupied to such a degree, that a local maximum of the density of states at the Fermi level is reached.

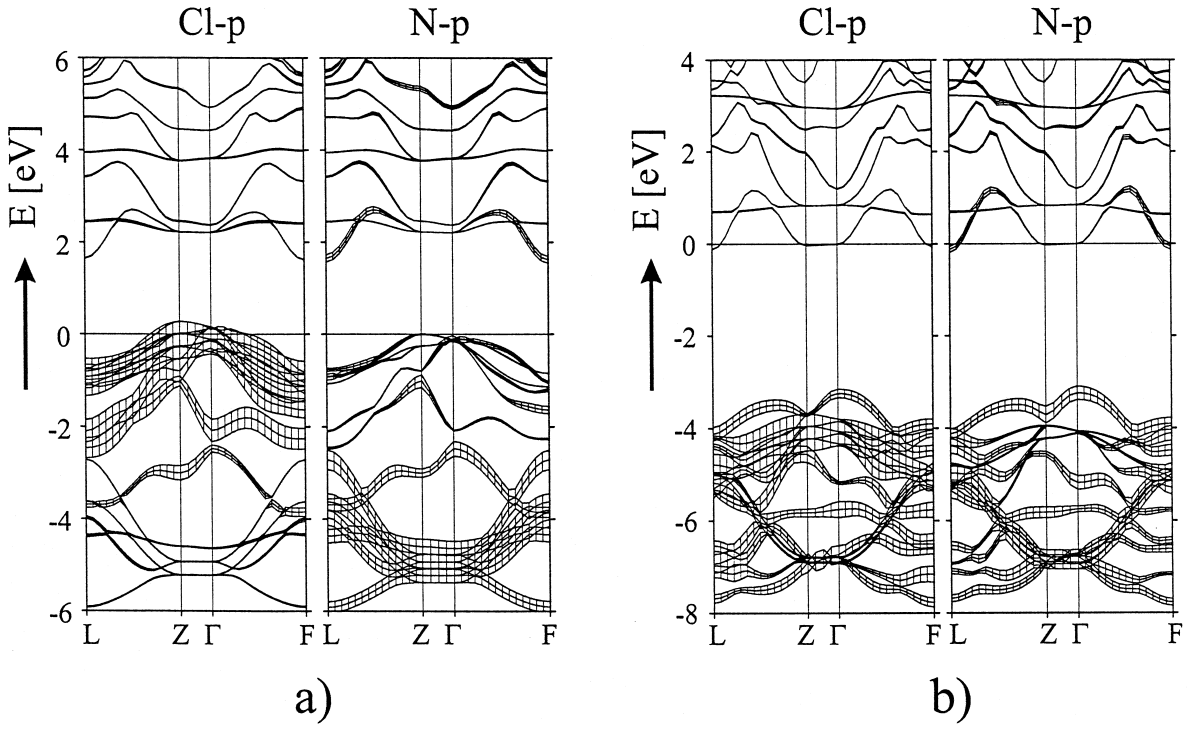

Fig. 6. Band structures on the basis of LMTO calculations of (a) ZrNCl and (b) $Li_{0.16}ZrNCl$ showing bands around the Fermi energy (0 eV). The fat band representation is given for the Cl-p and N-p contributions.

For a detailed analysis and a comparison of the electronic band structures of β-ZrNCl and $Li_{0.16}ZrNCl$, we have calculated the corresponding band structures using the self-consistent scalar relativistic LMTO method [26,27]. All *k*-space integrations were performed with the tetrahedron method using 32 *k* points within the Brillouin zone. The basis sets consisted of 5s and 4d for Zr, 2s and 2p orbitals for N and 3p for Cl. The 3s and the 4s orbitals as well as the 3s orbitals of N were dealt with the downfolding technique [26] treating the inner electrons as a soft core. It was necessary to fill the interatomic space by introducing the so-called interstitial empty spheres in such a way that space filling was achieved without exceeding an overlap of 18%. In order to avoid the appearance of a ghost band downfolding for the orbitals of the empty spheres had to be switched off in the calculation.

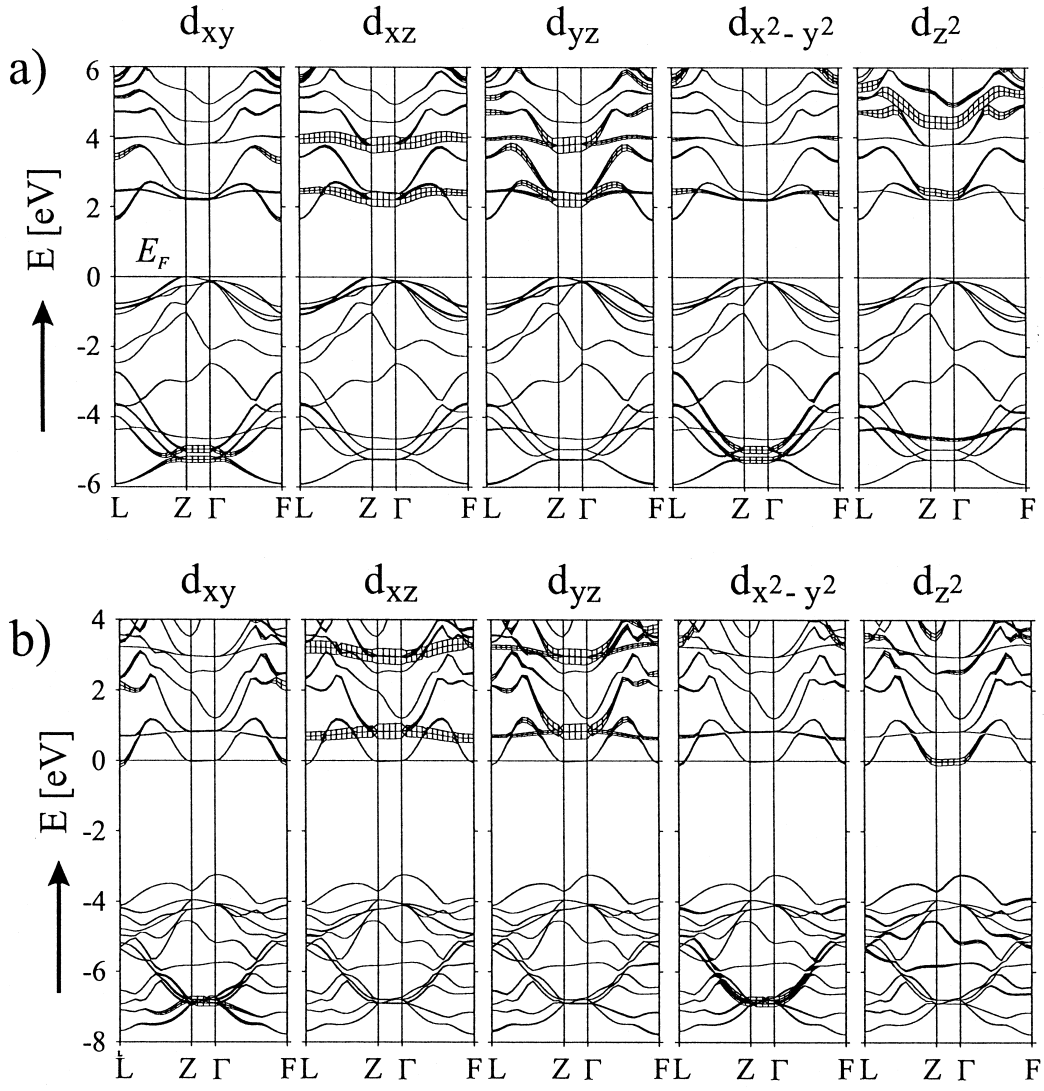

Fig. 7. Band structures on the basis of LMTO calculations of (a) ZrNCl and (b) $Li_{0.16}ZrNCl$ showing bands around the Fermi energy (0 eV). The fat band representation is given for the Zr-d contributions.

The calculated electronic band structures along some symmetry lines in the rhombohedral Brillouin zone for β-ZrNCl and $Li_{0.16}ZrNCl$ are shown in Figs. 6 and 7. In both cases, the Fermi level (E_F) has been chosen at zero energy and the fat band representation is given for the contributions of the contributing orbitals of the different atoms.

In β-ZrNCl, the bands below E_F down to -4 eV are mainly Cl-p centered and the N-p bands are lower in energy, at -4 eV to -6 eV. This result is not surprising because in contrast to the N atoms the Cl atoms are coordinated only on one side by three Zr atoms. There is a mixing of the '*in*'-plane orbitals Zr-d_{xy} and Zr-$d_{x^2-y^2}$ with the N-p states at -5 eV which reflects some stabilisation of the structure within the ZrN slabs, see Fig. 7a. The calculated band gap is approximately 2 eV. The Zr-d states, constituting the lowest unoccupied band, have two minima at L and F and, slightly higher in energy, a flat band part occurring between Γ and Z where the main contributions come from d_{xz}, d_{yz} and d_{z^2}. These states, like others, between Γ and Z show nearly no dispersion which is not surprising since β-ZrNCl has a sheet-like structure.

The band structure of $Li_{0.16}ZrNCl$ exhibits some significant differences compared to the band structure of β-ZrNCl, see Fig. 6b and Fig. 7b. The N-p and Cl-p states below E_F are both at the same energy between -4 eV and -8 eV as the Cl centered states are stabilised by the Li–Cl bonding between the Cl sheets. Like in β-ZrNCl we also find Zr contribution at approximately -5 eV to consist mainly d_{xz} and d_{yz} due to a fair overlap with the anion states. Furthermore, the conduction band in $Li_{0.16}ZrNCl$ has two minima at F and L slightly below the E_F, but the flat band part between Γ and Z lies nearly at the same energy and has a mainly Zr-d_{z^2} character. Recently, it has been proposed that the simultaneous occurrence of bands with greater dispersion, ''wide bands'', besides ''flat bands'' at E_F, which corresponds to a tendency towards pairwise localisation of electrons is a prerequisite for superconductivity [28,29]. The electronic band structure of $Li_{0.16}ZrNCl$ is in accordance with such a scenario. This still holds when the Fermi level is slightly raised by further intercalation of Li provided that no significant distortions of the structure will occur. However, when the Fermi level comes to lie significantly above the flat band part in the band structure superconductivity should be lost. Intercalation up to $Li_{0.5}ZrNCl$ leaves T_c nearly unchanged whereas a further increase of the Li content up to $Li_{1.4}ZrNCl$ leads to a decrease of T_c to 10 K [3]. The preservation of superconductivity hints to a non-rigid band structure. For a more detailed discussion it is necessary to have structural data available of a series of different compounds of the type Li_xZrNCl ($0 < x < 1.2$).

5. Conclusion

According to our Rietveld refinement, β-ZrNCl crystallises in the SmSI type structure containing 2D $[ClZr_2N_2Cl]$ slabs with the so-called 1s stacking. Li doping of β-ZrNCl leads to a shift of these slabs resulting in the superconducting 3s-Li_xZrNCl ($0 < x < 1.2$). The electronic band structure of Li_xZrNCl is characterised by a high density of states at the Fermi level which have Zr–Zr bonding and Zr–N antibonding character. Therefore, the nature of superconductivity in Li_xZrNCl is rather related to the 3D analogue ZrN than to copper-based superconductors.

Acknowledgements

The authors thank O. Jepsen for helpful discussions concerning the LMTO calculations and U. Kessler for the help with the collection of X-ray powder diffraction data. Dr. S.Ya. Istomin is also grateful to the Max-Planck-Gesellschaft for financial support.

References

[1] S. Yamanaka, K. Hotehama, H. Kawaji, M. Ohashi, Adv. Mater. 9 (1996) 771.
[2] S. Yamanaka, K. Hotehama, H. Kawaji, Nature 392 (1998) 580.
[3] H. Kawaji, K. Hotehama, S. Yamanaka, Chem. Mater. 9 (1997) 2127.
[4] R. Juza, J. Hendersen, Z. Anorg. Allg. Chem. 332 (1964) 159.
[5] M. Ohashi, S. Yamanaka, M. Sumihara, M. Hattori, J. Solid State Chem. 75 (1988) 99.
[6] R. Juza, H. Friedrichsen, Z. Anorg. Allg. Chem. 332 (1964) 173.
[7] A.M. Fogg, J.S.O. Evans, D. O'Hare, Chem. Commun. 20 (1998) 2269.
[8] S. Shamato, T. Kato, Y. Ono, M. Myazaki, K. Ohoyama, M. Ohashi, Y. Yamaguchi, T. Kajitani, Physica C 306 (1998) 7.
[9] A. Fuertes, M. Vlassov, D. Beltran-Perter, P. Alemany, E. Canadell, N. Casan-Pastor, M.R. Palacin, Chem. Mater. 11 (1999) 203.
[10] M. Ohashi, S. Yamanaka, Y. Morimoto, M. Hattori, Bull. Chem. Soc. Jpn. 60 (1987) 2387.
[11] M. Ohashi, S. Yamanaka, M. Hattori, J. Solid State Chem. 77 (1988) 342.
[12] M. Ohashi, H. Hakano, S. Yamanaka, M. Hattori, Solid State Ionics 31/32 (1989) 97.
[13] L.G. Akselrud, Yu.N. Grin, P. Yu. Pecharsky, V.S. Fundamentsky, Thesis report on the 12th ECM, Moscow, 1989, p. 155.
[14] CSD '94 Release, User manual, p. 124.
[15] D. Adolphson, J.D. Corbett, Inorg. Chem. 15 (1976) 1820.
[16] P.M. Woodward, T. Vogt, J. Solid State Chem. 138 (1998) 207.
[17] F. Ueno, K. Ziebeck, H.-J. Mattausch, A. Simon, Rev. Chim. Miner. 21 (1984) 804.
[18] M. Bäcker, A. Simon, R.K. Kremer, H.-J. Mattausch, R. Dronskowski, J. Rouxel, Angew. Chem., Int. Ed. Engl. 35 (1996) 752.
[19] C. Felser, R. Seshadri, J. Mater. Chem. 9 (1999) 459.
[20] R. Hoffmann, J. Chem. Phys. 39 (1963) 1397.
[21] J.H. Ammeter, H.B. Bürgi, J.C. Thibeault, R. Hoffmann, J. Am. Chem. Soc. 100 (1978) 3686.
[22] M.H. Whangbo, R. Hoffmann, J. Am. Chem. Soc. 100 (1978) 6093.
[23] R. Ramirez, M.C. Böhm, Int. J. Quantum Chem. 30 (1986) 391.
[24] R.H. Summerville, R. Hoffmann, J. Am. Chem. Soc. 98 (1976) 7240.
[25] J. Köhler, PC-Version of EHMACC (Extended-Hückel program, written by M.H. Whangbo, R. Hoffmann, modified by M. Evain, J. Mitchel), Stuttgart, 1991.
[26] O.K. Andersen, O. Jepsen, M. Snob, Linearized band-structure method in electronic band structure and its applications, Lecture Notes in Physics, Springer, Berlin, 1987.
[27] O.K. Andersen, O. Jepsen, Phys. Rev. Lett. 53 (1984) 2571.
[28] A. Simon, Angew. Chem., Int. Ed. Engl. 109 (1997) 1873.
[29] A. Simon, Angew. Chem., Int. Ed. Engl. 36 (1997) 1788.